International Microbiology (2023) 26:881–891
https://doi.org/10.1007/s10123-023-00343-3

RESEARCH

Abrogation of efflux pump activity, biofilm formation, and immune escape by candidacidal geraniol in emerging superbug, *Candida auris*

Tazeen Fatima[1] · Zeeshan Fatima[1,2] · Saif Hameed[1]

Received: 1 October 2022 / Revised: 7 February 2023 / Accepted: 16 February 2023 / Published online: 27 February 2023

Abstract

During the last decade, *Candida auris* emerged as a threatening human fungal pathogen that notably caused outbreaks around the globe with high mortality. Considering *C. auris* species as newly discovered fungi, the evolutionary features remain elusive. The antifungal resistance which is a norm in *C. auris* underlines the need for innovative therapeutic options. ATP Binding Cassette (ABC) superfamily efflux pumps overexpression and biofilms are known to be major contributors to multidrug resistance (MDR) in *C. auris*. Therefore, herein, we investigated the antifungal potential of geraniol (Ger) as a promising natural compound in the fight against MDR *C. auris*. Our experiments proved that Ger was fungicidal in nature and impaired rhodamine 6G (R6G) efflux, confirming the specific effect on ABC transporters. Kinetic studies unravelled the competitive mode of inhibition by Ger for R6G efflux since the apparent K_m increased with no change in V_{max} value. Mechanistic insights also revealed that Ger depleted ergosterol content in *C. auris*. Furthermore, Ger led to inhibition in biofilm formation as evident from crystal violet staining, biofilm metabolic and biomass measurements. Additionally, enhanced survival of *Caenorhabditis elegans* model after *C. auris* infection demonstrated the in vivo efficacy of Ger. Lastly, the in vivo efficacy was confirmed from a THP-1 cell line model which depicted enhanced macrophage–mediated killing in the presence of Ger. Modulation of *C. auris* efflux pump activity and biofilm formation by Ger represents a promising approach to combat MDR. Together, this study demonstrated the potential therapeutic insights of Ger as a promising addition to the antifungal armamentarium required to treat emerging and resistant *C. auris*.

Keywords *Candida* · MDR · Efflux pump · Ergosterol · Biofilm · *C. elegans* · Macropha

Introduction

More effective antifungal strategies are needed to fight against emerging and drug-resistant fungal infections (El-Baz et al. 2021). The introduction of techniques such as hematopoietic stem cell transplantation (HSCT) and new chemotherapeutic and immunomodulatory agents led to an increase in the population of immunocompromised patients which are particularly sensitive to invasive fungal infections.

✉ Zeeshan Fatima
drzeeshanfatima@gmail.com

✉ Saif Hameed
saifhameed@yahoo.co.in

[1] Amity Institute of Biotechnology, Amity University Haryana, Gurugram (Manesar) - 122413, India

[2] Department of Medical Laboratory Sciences, College of Applied Medical Sciences, University of Bisha, Bisha – 61922, Saudi Arabia

Yeasts, particularly from the *Candida* genus, are the most common cause of occurrence in fungal infections, leading to both superficial and invasive infections (Bilal et al. 2022). Even if many species are harmless commensals or endosymbionts of hosts including humans, they can turn pathogenic and cause opportunistic infections. Among *Candida* species, *Candida albicans* is the most isolated one. It is known to cause candidiasis or thrush in humans and animals. However, since its advent over a decade ago, *Candida auris* rapidly emerged as a global health threat (Satoh et al. 2009; Desnos-Ollivier et al. 2021). This is particularly due to its intrinsic resistance against most of the available antifungal therapeutics (Ruchti et al. 2022) unlike other *Candida* spp., including the prevalent *C. albicans* which develops resistance after long-term deployment of drugs by the different resistance mechanisms like overexpression of efflux pumps, enzymatic upregulation, and biofilm formation by a phenomenon known as multidrug resistance (MDR) (Tanwar et al. 2014). In addition, current antifungal drugs are associated

with limitations such as narrow antifungal spectrum, toxicity, and high cost of treatment (Lone et al. 2020). Thus, discovering novel antifungal agents that can combat MDR is of great impact.

In this scenario, given the limited armory of effective antifungals and considering that the development of new antifungals is time-consuming and involves huge economic investment, natural compounds of plant origin have been selected as a promising option due to their lower expected toxicity and cost-effectiveness. Therefore, great attention is being given to the search for phytotherapeutics. Geraniol (Ger) is a monoterpene alcohol found as a major component of geranium oil. The potential medicinal application of Ger is based on its pharmacological properties, including reported antimicrobial activities. Structurally, Ger is an acyclic terpene named as 3,7-dimethylocta trans-2,6-dien-1-ol. It is listed under GRAS (Generally Regarded As Safe) by the FDA (Food and Drug Administration) and Flavor and Extract Manufacturers Association (FEMA) (https://www.drugbank.ca/drugs/DB14183). Ger exhibited antibacterial, antihelmintic, anti-inflammatory, and anticarcinogenic activities (Singh et al. 2012; Abdel-Rahman et al. 2013; Zhu et al. 2014; Singulani et al. 2018; Misra et al. 2013). The antifungal potential of Ger against other *Candida* spp. including prevalent ones, viz., *C. albicans* and *C. glabrata*, has been reported from wide ranges of studies (Bard et al. 1988; Leite et al. 2015; Sharma et al. 2016; Singh et al. 2016; Gupta et al. 2021; Kaypetch et al. 2022) but no studies investigated the effects of Ger against *C. auris* and its virulence factors. In fact, considering the promising commercial and industrial value in medicine for Ger, *Candida glycerinogenes* was recently explored as a heterologous host for Ger production (Zhao et al. 2022). The present study aimed to explore the therapeutic benefits of Ger against *C. auris* with insight on its mode of action. With the background based on the aforementioned studies, the experiments emphasized the effects of Ger on growth, efflux pump activity, biofilm formation, and host pathogen interactions in *C. auris*.

Materials and methods

All medium chemicals, yeast extract (HiMedia) peptone (SRL) dextrose (Fisher Scientific) (YEPD), agar (Fisher Scientific), rhodamine 6G (R6G) (HiMedia), 2-deoxy glucose (2-DOG) (HiMedia), 2,4 dinitrophenol (2,4 DNP) (HiMedia), brain heart infusion (BHI) media (HiMedia/catalogue no. M210-500G), cholesterol (SRL), and ampicillin (HiMedia). Sodium chloride (NaCl) (Fisher Scientific), calcium chloride ($CaCl_2$) (Fisher Scientific), potassium chloride (KCl) (HiMedia), mannitol (Fisher Scientific), disodium hydrogen orthophosphate (Fisher Scientific), potassium dihydrogen orthophosphate (Fisher Scientific), dipotassium hydrogen orthophosphate (Fisher Scientific), sodium hydroxide (Fisher Scientific), d-glucose (Fisher Scientific), and dimethyl sulfoxide (DMSO) were obtained from Fischer Scientific. Crystal violet (CV), calcofluor-white (CFW), and geraniol (Ger) was obtained from Sigma Chemical Co. (St. Louis, MO, USA). N-Heptane was obtained from Central Drug House Pvt. Ltd., New Delhi. Thiazolyl blue (MTT) was obtained from Sisco Research Laboratories Pvt. Ltd., New Delhi.

Growth media and strain used

C. auris CBS10913T was used as the reference strain in this study and generously provided from the Department of Medical Microbiology, postgraduate Institute of Medical Education and Research, Chandigarh. YEPD broth with the composition of yeast extract 1% (w/v), peptone 2% (w/v), and dextrose 2 % (w/v), or for agar plates, 2% (w/v) agar, was used to grow the strain. Before conducting the experiments, we ensured to revive the strain either on YEPD broth or agar plate as applicable.

Antifungal susceptibility assays

Antifungal susceptibility was performed by determining minimal inhibitory concentration (MIC) and spot assay.

Minimum inhibitory concentration (MIC)

We followed the guidelines mentioned in method M27-A3 from the Clinical and Laboratory Standards Institute (CLSI) formerly NCCLS (National Committee for Clinical and Laboratory Standards 2008) to determine MIC by broth microdilution method. Briefly, 100 µl of YEPD media was added to each well of the 96-well plate followed by the addition of Ger and subsequently serially diluted. In total, 100 µl of cell suspension (in normal saline to an OD_{600} 0.1) was added to each well of the plate, and OD_{600} was measured after 48 h at 30 °C from a UV-visible 96-well plate reader (Genetix-GMB-580 Biotech Asia Pvt Ltd). The MIC_{90} was defined as the concentration at which at least 90% of the growth was inhibited.

Spot assay

Spot assays were performed using a drop dilution method as described previously (Singh et al. 2016). Briefly, for the spot assay, 5 µl of fivefold serial dilutions of *C. auris* (each with cells suspended in normal saline to an OD_{600} nm of 0.1) was spotted onto YEPD plates in the absence (control) and presence of Ger at subinhibitory concentration and growth difference was estimated after incubation at 30 °C for 48 h.

Static/cidal determination assay

In total, 0.1 OD_{600} *C. auris* cells were inoculated in the absence and presence of Ger at MIC incubated at 30 °C. On day 2, about 100-µl cultures were drawn and re-inoculated into the fresh YEPD media without Ger and further incubated for 24 h at 30°C. In the next day, OD_{600} was measured with a spectrophotometer (VSI Electronics Pvt Ltd/model no. VSI-501) to assess the static-cidal activity of Ger (Singh et al. 2018).

R6G extracellular efflux assay

The efflux pump activities were estimated by Rhodamine 6G (R6G) efflux as previously described (Singh et al. 2018; Hans et al. 2019). Yeast cell suspension was standardised according to McFarland Standards with the help of a spectrophotometer (VSI Electronics pvt ltd/model no. VSI-501) .About 1×10^6 yeast cells were inoculated to YEPD medium and allowed to grow for 5 h in the presence of Ger (65 µg/ml). Cells were harvested with phosphate-buffered saline (PBS) (without glucose), and resuspended as a 2% cell suspension, corresponding to 10^8 cells (wt/vol). The efflux pump activity was ceased by de-energizing for 45 min in 2-deoxy glucose (2-DOG) (5 mM) and 2,4 dinitrophenol (2,4 DNP) (5 mM) in PBS (without glucose). The de-energized cells were harvested again in PBS without glucose and R6G was added at a final concentration of 10 µM for further incubation of 40 min at 30 °C. The equilibrated cells were now harvested as a 2% cell suspension (wt/vol) in PBS with glucose at the indicated time. Withdrawn were 1-ml samples and centrifuged at 9000 *g* for 2 min. The supernatant was collected, and OD was measured at 527 nm. Glucose-free negative controls were also included in all the experiments. For competition assays, Ger (65µg/ml) was added to the de-energized cells 30 min before the addition of R6G at various concentrations (10 µM, 20 µM, 30 µM, 40 µM) and allowed to equilibrate to follow glucose for energy-dependent efflux as above.

Quantitation of ergosterol

The alcoholic KOH method was used to extract sterols and the percentage of ergosterol was calculated as previously described (Arthington-Skaggs et al. 1999; Singh et al. 2016). Briefly, 0.1 OD_{600} *C. auris* cells were inoculated in 50 ml of YEPD in the presence of Ger (65 µg/ml). The absorbance maxima for both ergosterol and 24(28)-DHE (dehydroergosterol) is at 281.5 nm, whereas only 24(28)-DHE absorbs at 230 nm. Hence, ergosterol content is determined by the difference in the amount of 24(28)-DHE (calculated from the OD_{230}) from the total ergosterol plus 24(28)-DHE content (calculated from the $OD_{281.5}$). Ergosterol content was calculated as a percentage of the wet weight of the cells with the following equations: % Ergosterol + % 24(28)-DHE = [(A281.5/290) × *F*] / pellet weight; % 24(28)-DHE = [(A230/518) × *F*] / pellet weight and % Ergosterol = [% ergosterol + % 24(28) DHE]—% 24(28) DHE, where *F* is the factor for dilution in petroleum ether and 290 and 518 are the *E* values (in percent per centimetre) determined for crystalline ergosterol and 24(28)-DHE, respectively.

Biofilm formation

Biofilm metabolic activity

For estimating biofilm metabolic activity (Saibabu et al., 2020), 50 µl (stock solution containing 5 mg/ml, diluted 1:5 in prewarmed 0.15 M PBS prior to addition) of tetrazolium salt, 3-[4, 5-dimethylthiazol-2-yl]-2, 5-diphenyltetrazolium bromide (MTT) was added in each well and incubated for 5 h at 37 °C. DMSO (200 µl) was added to each well to solubilize MTT formazan product, and OD was measured at 450 nm. The metabolic activity of biofilm was represented as absorbances.

Biofilm biomass quantification

Biofilm biomass was measured as described previously (Singh et al. 2018; Venkata et al. 2020). Bovine serum was used to treat the pre-weighed sterile silicone squares (1.5×1.5 cm; Sigma), for overnight, and washed with PBS before inoculation. *C. auris* cells from an exponential phase were diluted to an OD_{600} of 0.2 with Spider medium and added to a sterile 12-well plate having one prepared silicone square in each well. After incubation at 37 °C for 90 min with gentle agitation (150 rpm), we removed non-adherent cells by washing the squares with 2-ml PBS, and then transferring to a fresh 12-well plate containing 2-ml fresh Spider medium in the presence of Ger (65 µg/ml) to incubate at 37°C for an additional 60 h at 75 rpm agitation for biofilm formation. For dry mass measurements, the squares were washed in PBS, air dried, and weighed. The total biomass of each biofilm was calculated by subtracting the weight of the silicon square after biofilm formation from the pre-weighed silicon square.

C. elegans studies

C. elegans nematodes studies were performed according to the standard Kaplan-Meier method (Breger et al. 2007; Ansari et al. 2018). An NGM plate was used to grow the worms at 20°C, unless otherwise stated, and routinely maintained on *E. coli* OP50. About, 40 young adult hermaphrodite worms at L4 stage were transferred from a lawn of *E. coli* OP50 to BHI medium in the presence of Ger (65 µg/

ml). If the worms did not respond to the tapping on the plate, worms were considered dead and scored daily for 7 days. Each experimental condition was tested in triplicate. Nematode survival was plotted using the Kaplan-Meier method.

For the *C. elegans* co-infection liquid assay, methodology as described elsewhere was used (Breger et al. 2007; Ansari et al. 2018). Briefly, adult nematodes were pre-infected with *C. auris* for 2 h on BHI agar medium containing ampicillin (100 mg/ml). After incubation, 2 ml of sterile M9 buffer was used to wash the nematodes four times and collected by centrifugation at 900 rpm after each wash to pipette into wells of a 12-well microtitre dish (NEST Pvt Ltd) containing 2-ml liquid medium (20% BHI and 80% M9 buffer) in the presence of Ger (65 µg/ml). The infected *C. elegans* were incubated at 25°C for 7 days and scored as live or dead daily and images were taken on the 7th day of infection. Images were taken from a stereo microscope (Olympus, India) equipped with a Coslab camera at 10× magnification.

For visualization of intestinal persistence, *C. auris* lawns were prepared and worms were placed overnight, followed by washing with M9 buffer, and then pipetted onto OP50 seeded NGM plates. After 2 days, worms were again washed with M9 buffer and *C. auris*–fed *C. elegans* were stained with CFW. Fluorescence of CFW-stained *C. auris* was observed in the intestine of *C. elegans* through a fluorescence microscope (Nikon, Japan) at 100× magnification using NIS element software (Ansari et al. 2018).

Macrophage infection and killing assay

Roswell Park Memorial Institute (RPMI) 1640 medium with 10% fetal bovine serum (FBS) was used to maintain THP1-cell lines. For 48 h, 15 nM Phorbol 12-myristate 13-acetate (PMA) was used to treat the cells, and then washed three times. Prior to infection, a 1-ml culture of *C. auris* was pelleted for 2 min, reconstituted in RPMI 1640, vortexed for 2 min, and passed through a syringe (26 gauge needle) 2–3 times to remove cell clumping. THP-1–derived macrophages were infected with *C. auris* for 4 h at a multiplicity of infection ratio of 5:1 (pathogen: host), followed by treatment with amikacin (200 g/ml). The cells were rinsed with PBS and resuspended in RPMI supplemented with 10% FBS. Supernatants were collected after 24 h of infection and aspirated, and monolayers were gently washed three times with PBS. To determine the number of CFUs, 0.5% Triton–X was used to lyse the cells. The lysates were serially diluted in triplicate and plated on agar plates to determine CFUs as previously described (Singh et al. 2022; Hans et al. 2022).

Statistical analyses

All experiments were performed in triplicate ($n = 3$). The results are reported as mean ± standard deviation (SD) and analysed using Student's t test, wherein $P < 0.05$ was considered as statistically significant.

Results

Ger displays fungicidal activity against *C. auris*

The antifungal activity of Ger was tested against *C. auris* by broth microdilution assay to determine the MIC_{90}. Broth microdilution assay confirmed that Ger showed an antifungal effect against *C. auris* at MIC of 225 µg/ml (Fig. 1a). This result was further confirmed by the spot assay that corresponded with the broth microdilution assay (Fig. 1b). Furthermore, a spectrophotometric-based assay was performed to determine the static or cidal nature of Ger. We observed that growth was expectedly inhibited at MIC of Ger on the first day, but after re-inoculation on the second day, there was no growth of *C. auris* even in the absence of Ger (Fig. 1c), confirming its fungicidal nature. Additionally, being fungicidal, we needed to determine a Ger concentration that does not inhibit the growth considerably. Thus, for subsequent biochemical and phenotypic studies, Ger was used at a subinhibitory concentration of 65 µg/ml.

Ger competitively inhibits R6G efflux of ABC transporters in *C. auris*

To evaluate the effect of Ger on functionality of ATP Binding Cassette (ABC) superfamily transporters, we performed the R6G efflux assay. It was observed that *C. auris* showed functional efflux of R6G induced by glucose as depicted by extracellular concentration of the supernatant (Fig. 2a) contrary to impaired R6G efflux in presence of Ger with reduced extracellular R6G concentration (Fig. 2a). These observations were further confirmed by spot assay depicting no growth in the presence of R6G and Ger (Fig. 2b). Additionally, mechanistic insights into the mode of inhibition via Lineweaver-Burk plot revealed that R6G efflux was competitively inhibited by Ger, as the apparent Km increased from 58.15 to 124.94 while V_{max} remained unchanged (Fig. 2c). The rate of reaction was higher in Ger as the slope is steeper (Fig. 2c).

Ger confers ergosterol depletion in *C. auris*

Next, the effect of Ger on membrane composition of *C. auris* was studied and the ergosterol content in the presence of Ger using a UV spectrophotometer (VSI Electronics Pvt Ltd/model no. VSI-501) was quantified. Both ergosterol and 24(28)-DHE showed absorbance maxima at 281.5 nm while only 24(28)-DHE exhibited an absorbance maximum at 230 nm. Thus, we determined the ergosterol content by

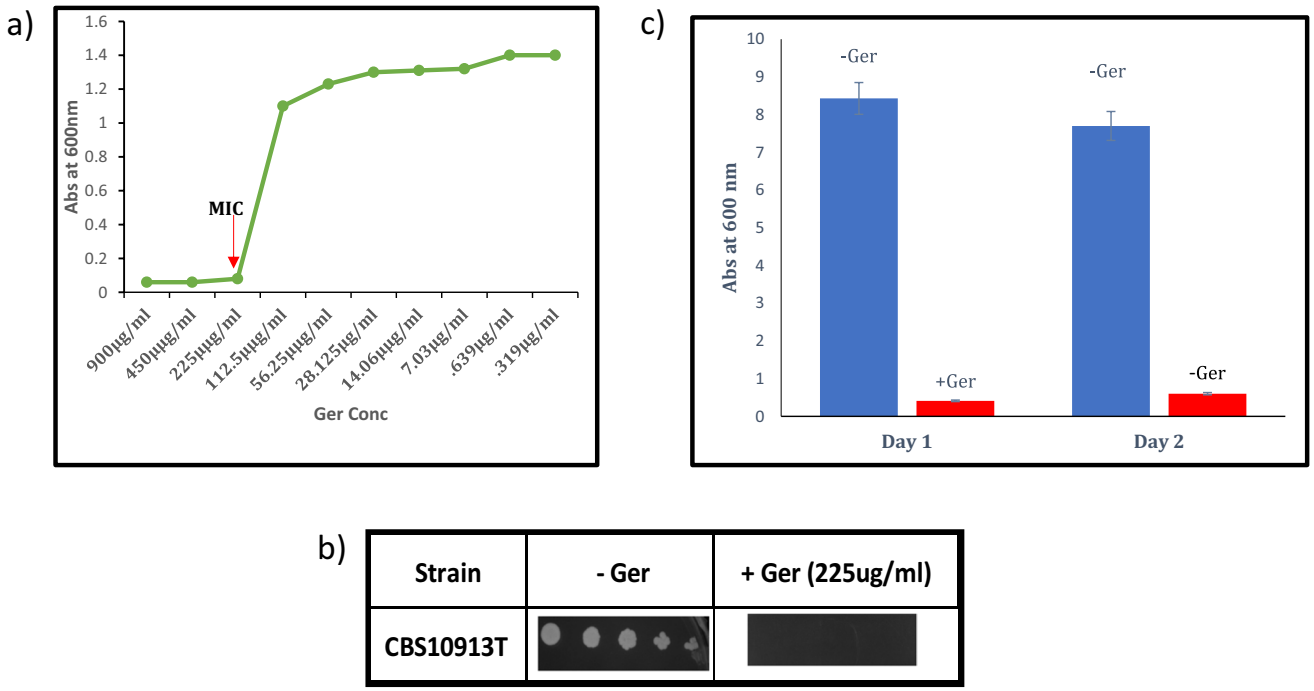

Fig. 1 Antifungal activity of Ger. **a** Broth microdilution assay to determine the MIC_{90} of *C. auris* in the presence of Ger. The y-axis depicts the absorbance measured at 600 nm and x-axis depicts the Ger concentrations in µg/ml. The minimum Ger concentration that inhibits growth by 90% relative to the drug-free growth control is indicated as MIC_{90}. **b** Spot assay of *C. auris* in the absence (-Ger) and presence of Ger (+Ger). **c** Bar graph depicting the revival of untreated *C. auris* cells (-Ger) and non-revival of Ger-treated (MIC_{90}) cells in YEPD media confirming the fungicidal nature of Ger

calculating the difference of total ergosterol and 24(28)-DHE absorbance at 281.5 nm with only 24(28)-DHE absorbance at 230 nm. We found that ergosterol level was considerably decreased by 86% in the presence of Ger (Fig. 3).

Ger impairs biofilm formation in *C. auris*

Furthermore, the effect of Ger on biofilm formation of *C. auris* was studied. Firstly, visualization of biofilm-forming ability was assessed by qualitative CV staining. This series of experiments depicted clear disruption of biofilm formation (Fig. 4a). Next, the metabolic activity of biofilms was estimated using the MTT assay. The metabolic activity was considerably reduced by 75% in the presence of Ger, confirming inhibition in biofilm formation (Fig. 4b). Finally, biofilm biomass was measured, and it was observed that the biomass of biofilm formed in the presence of Ger was substantially lesser by 85% (Fig. 4c).

Ger enhances the survival of *C. auris*–infected *C. elegans*

Subsequently, the ability of Ger to prolong survival and reduction in the fungal burden of infected *C. elegans* was assessed. Firstly, the host toxicity of Ger was evaluated in the nematode model at its subinhibitory concentration (65 µg/ml) and we found that there was no considerable difference in growth between the untreated (60%) and treated worms (55%) until 7 days (Fig. 5a). Next, for investigating the antifungal effect, the worms were exposed to *C. auris* in the absence and presence of Ger. It was observed that the survival of *C. elegans* was enhanced considerably from 25 to 45% in the presence of Ger (Fig. 5b). Additionally, CFW staining of *C. auris*–infected *C. elegans* was performed and blue fluorescence was clearly depicted in the intestinal region of untreated contrary to the Ger-treated cells which displayed diminished fluorescence (Fig. 5c).

Ger impedes immune escape by enhanced macrophage–mediated killing of *C. auris*

Encouraged by these findings, the killing of intracellular yeast was further examined by employing THP-1 cells derived macrophages infected by *C. auris*. The growth inside the macrophages was assessed indirectly by determining the colony-forming units (CFU) to estimate phagocytosis mediated by macrophage killing. We found that the CFU post 24-h infection with Ger-treated *C. auris* displayed around

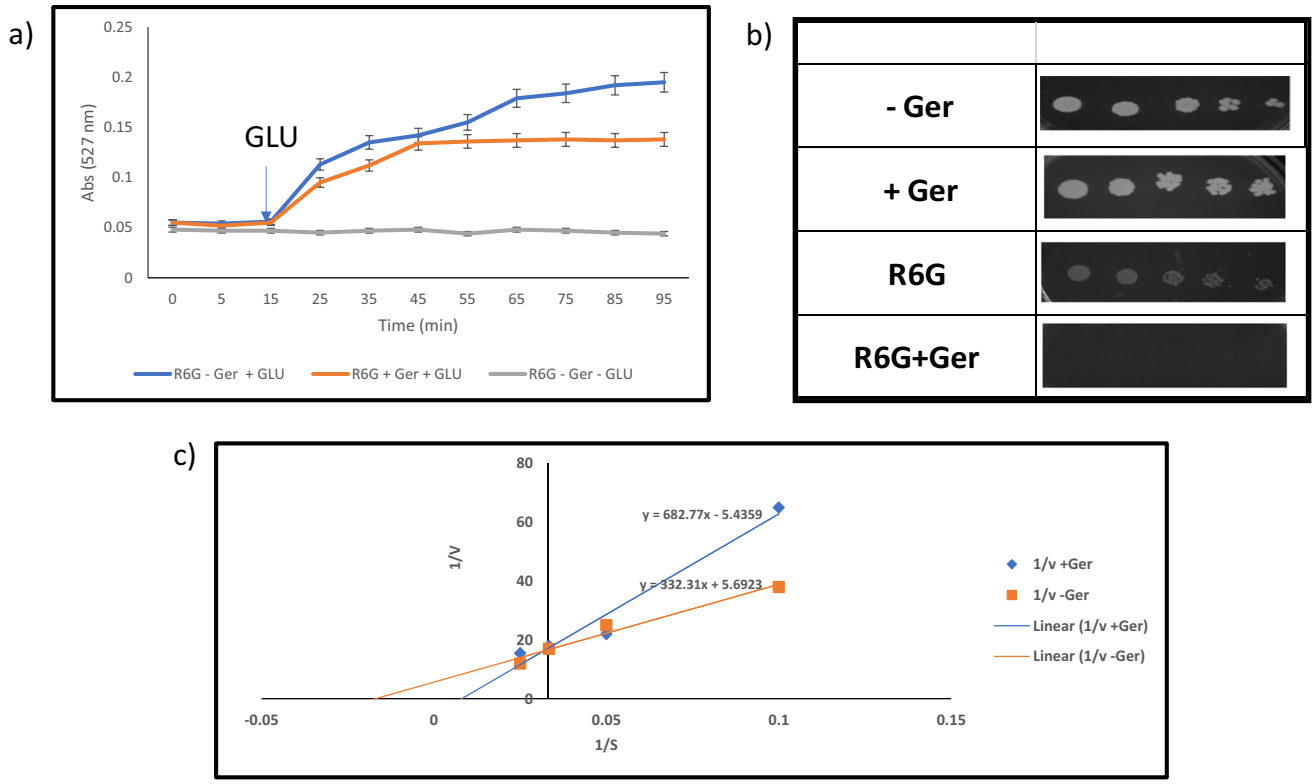

Fig. 2 Effect of Ger on R6G efflux. **a** Extracellular R6G concentrations in control cells (-Ger) and in the presence of Ger (+Ger). The energy-dependent R6G efflux was initiated by adding glucose (2%; indicated by an arrow) and quantified by measuring the absorbance of the supernatant at 527 nm. The values are the means and standard deviations (indicated by error bars) from three independent experiments. **b** Spot assay of *C. auris* in the presence and absence of Ger and R6G. **c** Lineweaver-Burk plot of R6G efflux in the absence (-Ger) and presence of Ger (+Ger). The x-axis (1/S) represents the various concentrations (µM) of R6G, and the y-axis (1/V) represents the rate of release of R6G in the presence of Ger (65 µg/ml)

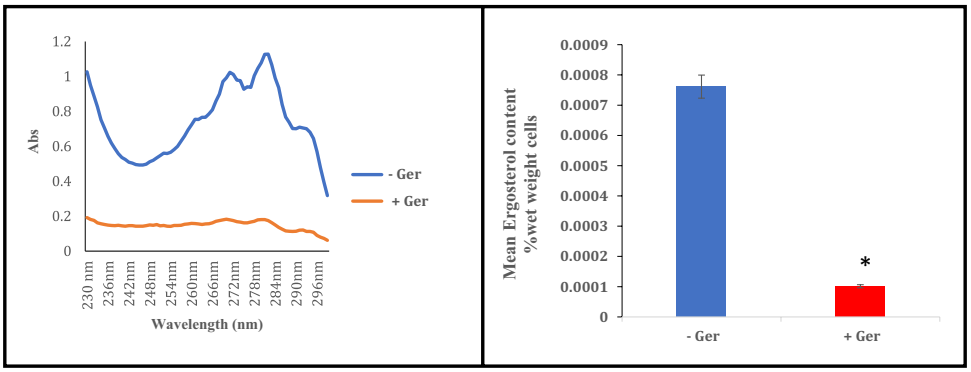

Fig. 3 Effect of Ger on ergosterol. The left panel depicts UV spectrophotometric ergosterol profiles of *C. auris* scanned between 220 and 300 nm from a culture grown for 16 h in the absence (-Ger) and presence of Ger (+Ger). The right panel depicts relative percentages of ergosterol content in the absence (control) and presence of Ger (65 µg/ml). Mean of % ergosterol levels is calculated as described in "Materials and methods" normalized by considering the untreated control as 100 ± SD of three independent sets of experiments is depicted on the y-axis and * depicts *P* value <0.05

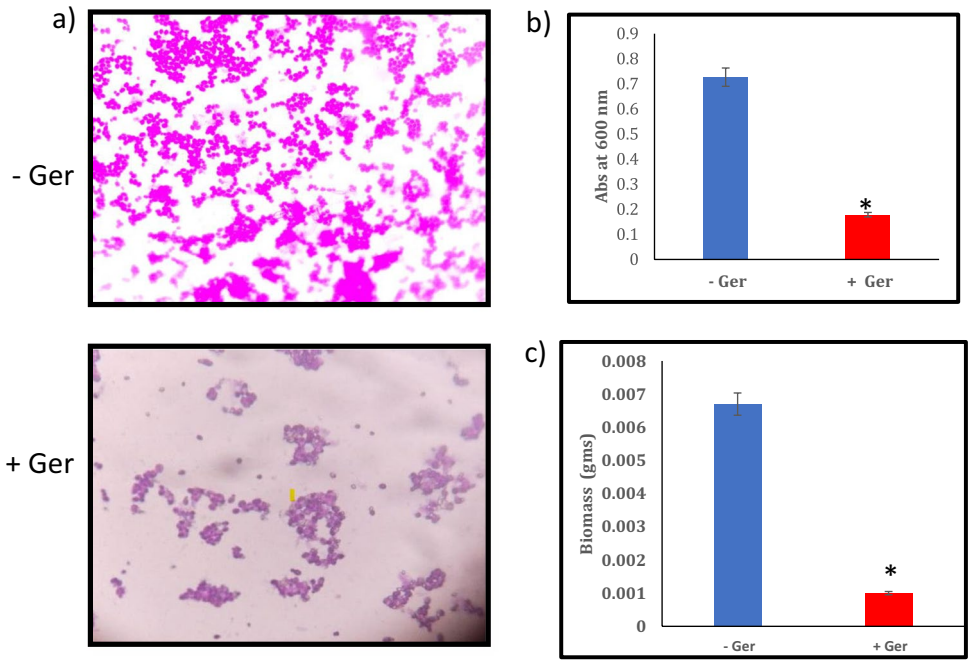

Fig. 4 Effect of Ger on biofilm formation of *C. auris*. **a** CV staining, as described in "Materials and methods," showing the biofilm formation in absence (-Ger) and presence of Ger (+Ger). **(b)** Effect of Ger on biofilm metabolic activity depicted as bar graph and quantified by using MTT assay as described in "Materials and methods." Mean of $O.D_{450}$ nm ± SD of three independent sets of experiments is depicted on the y-axis and * depicts *P* value <0.05. **c** Effect of Ger on biofilm biomass formed on silicone sheets. Mean of dry weight ± SD of three independent sets of experiments is depicted on the y-axis and * depicts $P < 0.05$

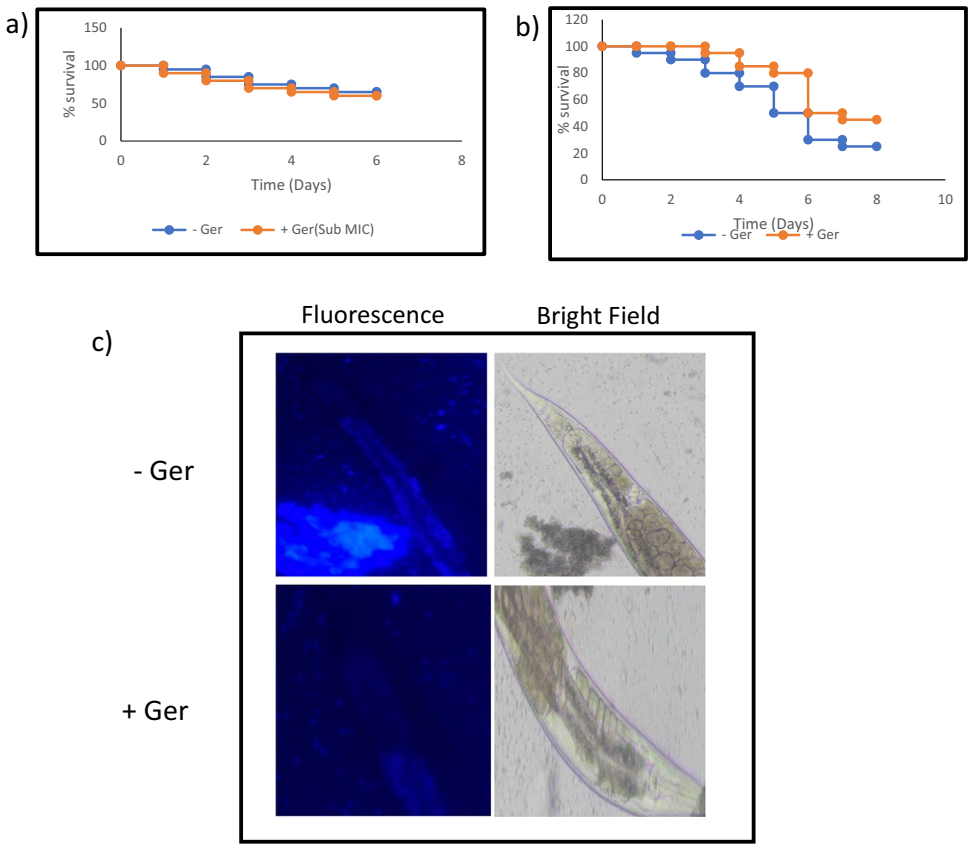

Fig. 5 In vivo studies of Ger on nematode model *C. elegans*. **a**Toxicity test of Ger on *C. elegans* depicted by the Kaplan–Meier curve showing % survival of *C. elegans* in the presence of Ger at sub-MIC concentration. Worm survival was determined based on movement. The toxicity of Ger was studied on nematodes by determining survival rates until 7 days. **b** Ger prolongs the survival of *C. albicans*–infected *C. elegans*. Kaplan–Meier curve showing % survival of *C. albicans*–infected *C. elegans* in the presence of Ger until 7 days. **c** Intestinal persistence of *C. auris* represented by the CFW-stained *C. auris* visualized in intestine of *C. elegans* treated with Ger showing lesser fungal burden. Magnification 100×

100 CFU log 10^5/ml in comparison to control cells which displayed almost 250 CFU log 10^5/ml (Fig. 6a). The images of the CFU after 24-h infection also confirmed the differences (Fig. 6b).

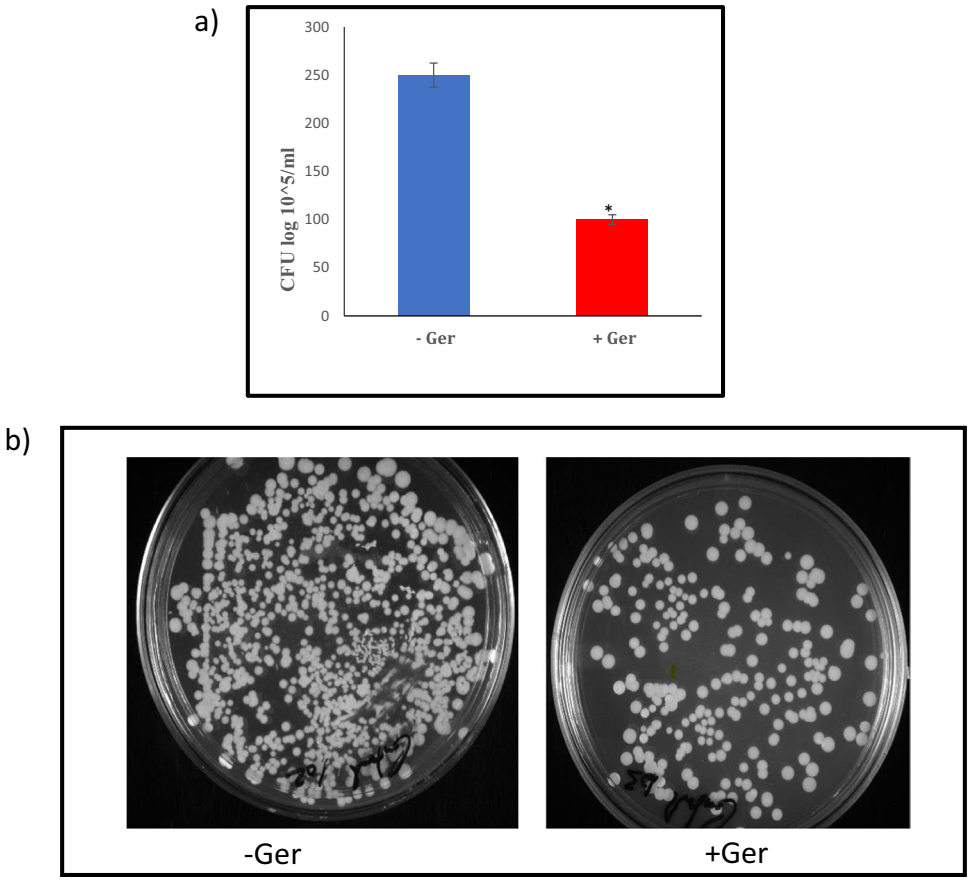

Fig. 6 Effect of Ger on macrophage killing ability. **a** Bar graph represents CFU log10^5/ml on the y-axis after 24-h infection with control (-Ger) and Ger-treated (+Ger) *C. auris* depicting the killing of fungi by macrophages. Data are expressed as mean ± SD of three independent sets of experiments. **b** CFU image of control (-Ger) and Ger-treated (+Ger) *C. auris* after 24-h infection. Magnification 40×

Discussion

Human fungal infections particularly those caused by *Candida* spp. gradually represent an alarming threat to public health. Even if *C. albicans* remain the most prevalent species, a shift in research focus was observed with the advent of *C. auris*. This fungus is posing significant challenges to microbiologists and clinicians because of (i) its natural intrinsic antifungal resistance, (ii) its ease of transmission from person to person in health care settings, and (iii) its misidentification by standard biochemical identification systems as *Candida haemulonii* due to a lack of *C. auris* in the databases (Chowdhary et al. 2017; Sanyaolu et al. 2022). Under such compelling circumstances, with its drug resistance, transmissibility, and severe outcomes, *C. auris* has all the features of a "superbug" and it becomes pertinent to identify new antifungals or new therapeutic strategies. Recently, there has been considerable scientific interest in the essential oils and their components as they represent a safe alternative with lesser side effects (El Baz et al. 2021; Zuzarte et al. 2022). In pursuit of searching effective therapeutics against the emerging superbug, *C. āuris*, the current study elucidated the antifungal mechanism of Ger, a natural monoterpenoid alcohol.

We proved that Ger depicted potent antifungal activity against *C. auris* which was displayed by its low MIC of 225 µg/ml (Fig. 1a and b). Ger's mode of action was identified as fungicidal at its MIC (Fig. 1c). Even if very few natural terpenoids exhibited cidal activities, ibrexafungerp was recently reported as the first triterpenoid antifungal with fungicidal profile (Sucher et al. 2022). To gain mechanistic insights into the mode of action of Ger, we first investigated the prominent mechanisms. Among them, overexpression of transporters belonging to ABC superfamily along with ergosterol biosynthesis gene, *ERG11*, is the main mechanisms responsible for MDR in *Candida* spp. (Whaley et al. 2017: Banerjee et al. 2022). In fact, in the genome of *C. auris*, at least 20 transmembrane domains are encoded by the genes associated with ABC transporters causing azole resistance (Wasi et al. 2019). Hence, we studied the functionality of ABC transporters by using its widely used substrate R6G-driven efflux. The result confirmed that extracellular concentration of R6G was reduced in the presence of Ger, suggesting that efflux pump activity of ABC transporters was impaired (Fig. 2a). This observation was further authenticated by spot assay as no growth in R6G-treated cells in the presence of Ger was measured (Fig. 2b). Additionally, we explored that the mode of inhibition by Ger was competitive in nature as the V_{max} value remained unchanged while K_m

increased (Fig. 2c). In the same context, the ergosterol content was quantified and considerably decreased in the presence of Ger (Fig. 3). Although still inconclusive, one may hypothesise that impaired efflux activity of ABC transporters could be due to lowering in ergosterol content as ABC transporters are known to preferentially localize in lipid raft regions which are rich in ergosterol (Pasrija et al. 2008) and we observed depleted ergosterol in the current study. Since identification of molecules that can modulate efflux pumps against *C. auris* is a highly topical matter, Ger could be a noteworthy finding.

It is already documented that nature is an admirable source for new bioactive compounds that can inhibit the pathogens associated with biofilm formation (Lu et al. 2019). If not efficiently managed, fungal infections can lead to serious consequences as fungi can colonize on hospital-associated devices such as catheters, dentures, and prosthetic joints (Tsui et al. 2016). Additionally, it also forms a protective barrier to both antifungal drugs and phagocytes thereby establishing as significant virulence trait (Roscetto et al. 2018). This study also demonstrated the capacity of Ger to suppress *C. auris* biofilm formation. We found that Ger considerably inhibits the biofilm formation as established by staining visualization (Fig. 4a), measuring the metabolic activity (Fig. 4b) and biomass (Fig. 4c) of biofilms.

Lastly, we demonstrated the in vivo efficacy of Ger by using two models namely *C. elegans* and THP-1 cell lines. Firstly, the result from the *C. elegans* demonstrated the non-toxic nature of Ger that did not exhibit any toxicity to the worms (Fig. 5a). Additionally, from the survival assay, it was apparent that in vivo colonization and virulence of *C. auris* were discernibly decreased in the presence of Ger (Fig. 5b). Furthermore, diminished CFW fluorescence clearly indicate that Ger reduced the intestinal persistence of *C. albicans* in *C. elegans* (Fig. 5c). Similarly, the host-pathogen interaction is known to establish the course of systemic *C. auris* disease. For the host defence against invading fungi, activated macrophages play a primary role as main reservoirs for intracellular pathogens. The induction of phagocytosis by activated macrophage-mediated killing as defence response is well known (Marodi L et al. 1991; Torres and Balish 1997). In our study, we observed that phagocytosis mediated by macrophage killing in the presence of Ger was enhanced as revealed by low CFU suggesting the low infectivity of Ger-treated *C. auris* (Fig. 6). These observations establish that Ger impedes the immune escape mechanisms of *C. auris*.

Conclusion

Considering the dominant impact of efflux in *C. auris* drug resistance, searching for inhibitors/modulators of efflux pumps represents a safer tool to combat MDR. Besides, the inhibitory effect on biofilm formation can be helpful to mitigate colonization on hospital-associated devices. Overall, this study represents a promising potential of novel antifungal compounds (Fig. 7); however, it warrants further investigations such as in vivo mouse studies.

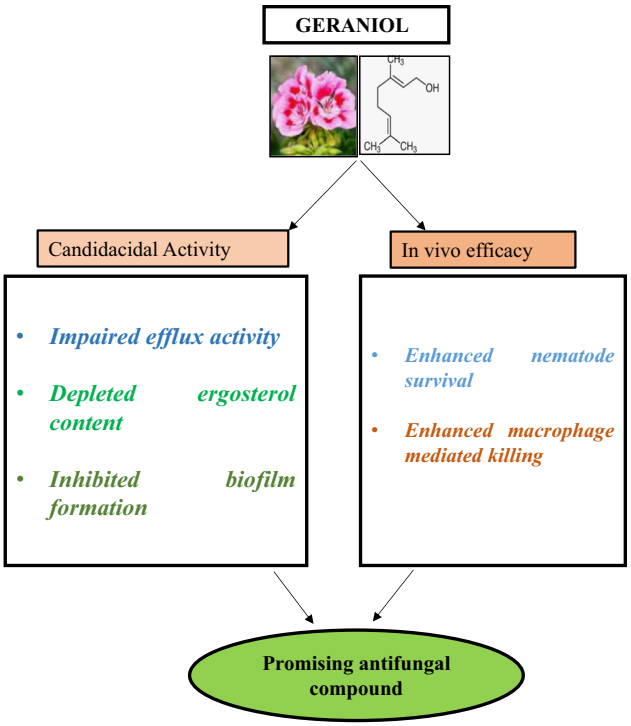

Fig. 7 Summary of anticandidacidal mode of action for Ger against *C. auris*

Acknowledgements We are grateful to Arunaloke Chakrabarty and Ramandeep Singh for providing the *C. auris* strain and THP-1 cell lines as generous gifts respectively. We thank Anindya Ghosh Roy, for providing wild-type *C. elegans*(N2) and *Escherichia coli* OP50. We thank Central Instrumentation Research Facility (CIRF), Amity University Haryana, for facilitating fluorescence microscopy. We also thank Rajendra Prasad, Dean Research, Amity University Haryana, for providing the available facilities for research in the institute. We acknowledge Muriel Billamboz for her assistance in English-language editing.

Author contributions TF: performed the experiment and data analysis. ZF and SH: supervision. TF: writing, original draft. ZF and SH contributed to the conception and design of the study, and review and editing of the manuscript.

Data Availability All the data generated in the study is within the manuscript.

Declarations

Ethics approval Not applicable.

Conflict of interest The authors declare no competing interests.

References

Abdel-Rahman FH, Alaniz NM, Saleh MA (2013) Nematicidal activity of terpenoids. J Environ Sci Health B 48:16–22

Ansari MA, Fatima Z, Ahmad K, Hameed S (2018) Monoterpenoid perillyl alcohol impairs metabolic flexibility of Candida albicans by inhibiting glyoxylate cycle. Biochem Biophys Res Commun. 495:560–566

Arthington-Skaggs BA, Jradi H, Desai T, Morrison CJ (1999) Quantitation of ergosterol content: novel method for determination of fluconazole susceptibility of Candida albicans. J Clin Microbiol 37(10):3332–3337

Banerjee A, Vishwakarma P, Meena NK, Lynn AM, Prasad R (2022) Bioinformatic identification of ABC transporters in Candida auris. Methods Mol Biol 2517:229–240

Bard M, Albrecht MR, Gupta N, Guynn CJ, Stillwell W (1988) Geraniol interferes with membrane functions in strains of Candida and Saccharomyces. Lipids 23(6):534–538. https://doi.org/10.1007/BF02535593

Bilal H, Shafiq M, Hou B, Islam R, Khan MN, Khan RU, Zeng Y (2022) Distribution and antifungal susceptibility pattern of *Candida* species from mainland China: a systematic analysis. Virulence 13(1):1573–1589

Breger J, Fuchs BB, Aperis G, Moy T, Ausubel FM, Mylonakis E (2007) Antifungal chemical compounds identified using a *C. elegans* pathogenicity assay. PLoS Pathog 3:e18

Chowdhary A, Sharma C, Meis JF (2017) Candida auris: a rapidly emerging cause of hospital-acquired multidrug-resistant fungal infections globally. PLoS Pathog. 13(5):e1006290

Desnos-Ollivier M, Fekkar A, Bretagne S (2021) Earliest case of Candida auris infection imported in 2007 in Europe from India prior to the 2009 description in Japan. J Mycol Med 31(3):101139

El-Baz AM, Mosbah RA, Goda RM, Mansour B, Sultana T, Dahms TES, El-Ganiny AM (2021) Back to nature: combating *Candida albicans* biofilm, phospholipase and hemolysin using plant essential oils. Antibiotics (Basel) 10(1):81

Gupta P, Gupta H, Poluri KM (2021) Geraniol eradicates Candida glabrata biofilm by targeting multiple cellular pathways. Appl Microbiol Biotechnol 105(13):5589–5605

Hans S, Fatima Z, Hameed S (2019) Magnesium deprivation affects cellular circuitry involved in drug resistance and virulence in Candida albicans. J Glob Antimicrob Resist 17:263–275. https://doi.org/10.1016/j.jgar.2019.01.011

Hans S, Fatima Z, Ahmad A, Hameed S (2022) Magnesium impairs Candida albicans immune evasion by reduced hyphal damage, enhanced β-glucan exposure and altered vacuole homeostasis. PLoS One 17(7):e0270676

Kaypetch R, Rudrakanjana P, Churnjitapirom P, Tua-Ngam P, Tonput P, Tantivitayakul P (2022) Geraniol and thymoquinone inhibit Candida spp. biofilm formation on acrylic denture resin without affecting surface roughness or color. J Oral Sci 64(2):161–166

Leite MC, de Brito Bezerra AP, de Sousa JP, de Oliveira LE (2015) Investigating the antifungal activity and mechanism(s) of geraniol against Candida albicans strains. Med Mycol 53:275–284

Lone SA, Khan S, Ahmad A (2020) Inhibition of ergosterol synthesis in Candida albicans by novel eugenol tosylate congeners targeting sterol 14α-demethylase (CYP51) enzyme. Arch Microbiol 202(4):711–726. https://doi.org/10.1007/s00203-019-01781-2

Lu L, Hu W, Tian Z, Yuan D, Yi G, Zhou Y, Cheng Q, Zhu J, Li M (2019) Developing natural products as potential anti-biofilm agents. Chin Med. 14:11

Maródi L, Forehand JR, Johnston RB Jr (1991) Mechanisms of host defense against Candida species. II. Biochemical basis for the killing of Candida by mononuclear phagocytes. J Immunol 146(8):2790–2794

Misra LN, Wouatsa NA, Kumar S, Venkatesh Kumar R, Tchoumbougnang F (2013) Antibacterial, cytotoxic activities and chemical composition of fruits of two Cameroonian Zanthoxylum species. J Ethnopharmacol 148:74–80

National Committee for Clinical and Laboratory Standards (2008) Reference method for broth dilution antifungal susceptibility testing of yeasts, Approved standard M27-A3. National Committee for Clinical and Laboratory Standards, Wayne, PA, p 14

Pasrija R, Panwar SL, Prasad R (2008) Multidrug transporters CaCdr1p and CaMdr1p of Candida albicans display different lipid specificities: both ergosterol and sphingolipids are essential for targeting of CaCdr1p to membrane rafts. Antimicrob Agents Chemother 52(2):694–704

Roscetto E, Contursi P, Vollaro A, Fusco S, Notomista E, Catania MR (2018) Antifungal and anti-biofilm activity of the first cryptic antimicrobial peptide from an archaeal protein against Candida spp. clinical isolates. Sci Rep 8(1):17570

Ruchti F, LeibundGut-Landmann S (2022) New insights into immunity to skin fungi shape our understanding of health and disease. Parasite Immunol 45(2):e12948

Sanyaolu A, Okorie C, Marinkovic A, Abbasi AF, Prakash S, Mangat J, Hosein Z, Haider N, Chan J (2022) *Candida auris*: an overview of the emerging drug-resistant fungal infection. Infect Chemother 54(2):236–246

Satoh K, Makimura K, Hasumi Y, Nishiyama Y, Uchida K, Yamaguchi H (2009) Candida auris sp. nov., a novel ascomycetous yeast isolated from the external ear canal of an inpatient in a Japanese hospital. Microbiol Immunol 53(1):41–44

Sharma Y, Khan LA, Manzoor N (2016) Anti-Candida activity of geraniol involves disruption of cell membrane integrity and function. J Mycol Med 26(3):244–254

Singh D, Kumar TR, Gupta VK, Chaturvedi P (2012) Antimicrobial activity of some promising plant oils, molecules and formulations. Indian J Exp Biol 50:714–717

Singh S, Fatima Z, Ahmad K, Hameed S (2018) Fungicidal action of geraniol against Candida albicans is potentiated by abrogated CaCdr1p drug efflux and fluconazole synergism. PLoS One 13(8):e0203079

Singh S, Fatima Z, Hameed S (2016) Insights into the mode of action of anticandidal herbal monoterpenoid geraniol reveal disruption of multiple MDR mechanisms and virulence attributes in Candida albicans. Arch Microbiol 198(5):459–472

Singh S, Hans S, Ahmad A, Fatima Z, Hameed S (2022) Unique roles of aminophospholipid translocase Drs2p in governing efflux pump activity, ergosterol level, virulence traits, and host-pathogen interaction in Candida albicans. Int Microbiol 25(4):769–779

Singulani JL, Pedroso RS, Ribeiro AB, Nicolella HD, Freitas KS, Damasceno JL, Vieira TM, Crotti AE, Tavares DC, Martins CH, Mendes-Giannini MJ, Pires RH (2018) Geraniol and linalool anticandidal activity, genotoxic potential and embryotoxic effect on zebrafish. Future Microbiol 13:1637–1646

Sucher AJ, Thai A, Tran C, Mantena N, Noronha A, Chahine EB (2022) Ibrexafungerp: A new triterpenoid antifungal. Am J Health Syst Pharm 79(24):2208–2221

Tanwar J, Das S, Fatima Z, Hameed S (2014) Multidrug resistance: an emerging crisis. Interdiscip Perspect Infect Dis 2014:1–7. https://doi.org/10.1155/2014/541340

Tsui C, Kong EF, Jabra-Rizk MA (2016) Pathogenesis of Candida albicans biofilm. Pathog Dis 74(4):ftw018

Vázquez-Torres A, Balish E (1997) Macrophages in resistance to candidiasis. Microbiol Mol Biol Rev 61(2):170–192

Venkata S, Zeeshan F, Kamal A, Luqman AK, Saif H (2020) Efficiency of vanillin in impeding metabolic adaptability and virulence of *Candida albicans* by inhibiting glyoxylate cycle, morphogenesis, and biofilm formation. Curr Med Mycol 6(1):1–8

Wasi M, Khandelwal NK, Moorhouse AJ, Nair R, Vishwakarma P, Bravo Ruiz G, Ross ZK, Lorenz A, Rudramurthy SM, Chakrabarti A, Lynn AM, Mondal AK, Gow NAR, Prasad R (2019) ABC transporter genes show upregulated expression in drug-resistant clinical isolates of *Candida auris*: a genome-wide characterization of ATP-Binding Cassette (ABC) transporter genes. Front Microbiol 10:1445

Whaley SG, Berkow EL, Rybak JM, Nishimoto AT, Barker KS, Rogers PD (2017) Azole antifungal resistance in *Candida albicans* and emerging Non-*albicans Candida* species. Front Microbiol. 7:2173

Zhao C, Wang XH, Lu XY, Zong H, Zhuge B (2022) Tuning geraniol biosynthesis via a novel decane-responsive promoter in *Candida glycerinogenes*. ACS Synth Biol 11(5):1835–1844

Zhu JJ, Brewer GJ, Boxler DJ (2014) Comparisons of antifeedancy and spatial repellency of three natural product repellents against horn flies, Haematobia irritans (Diptera: Muscidae). Pest Manag Sci 71(11):1553–1560. https://doi.org/10.1002/ps.3960

Zuzarte M, Salgueiro L (2022) Essential oils in respiratory mycosis: a review. Molecules 27(13):4140